ROBUSTNESS ANALYSIS OF AMB SUSPENSION

Erkki Lantto,[1] Matti Antila,[1] Ville Tommila[1]

ABSTRACT

This paper deals with the robustness analysis of the active magnetic bearing suspension. First, finite element method is used to find the variations of the bearing parameters. Based on this analysis, a plant description is proposed, where the uncertainties are modeled as uncertain "almost" diagonal and real gain matrices. For the robustness analysis, a special way of constructing a generalized Nyquist diagram is proposed. This diagram gives nonconservative stability margin predictions and is a useful tool for synthesis purposes. Finally, the test machine is analyzed using the proposed method.

1 INTRODUCTION

Even thought active magnetic bearing (AMB) suspension is open loop unstable, it is usually quite easy to achieve stable suspension at some nominal conditions. However, when the AMB is designed for series production, the situation becomes difficult. The performance demands are high and the one and only control system should handle all the machines operating at different operational conditions and having slightly different parameters due to manufacturing tolerances. Careful testing and powerful analysis tools are needed to ensure robustness.

There are many kinds of AMB applications and accordingly the most important performance objectives and parameter variations are different. Fittro et al. (1996) have successfully used μ-synthesis to achieve a controller for spindle AMB. Worst case point compliance minimization in the case of elastic rotor is an extremely challenging task in which very powerful synthesis method is needed. This particular application field is suitable for μ-synthesis also because the performance objective is clear and easy to formulate mathematically. The μ-synthesis, however, leads to high order controllers and in many easier applications the performance and robustness increase is only marginal compared with a well designed low order controller.

In the subcritical low pressure compressor applications (Antila et al., 1996), such as our test machine, the performance demands can not be formulated so easily into mathematical form. The main demand is that machines tolerates well all the disturbances and rotates smoothly in

[1]Helsinki University of Technology, Laboratory of Electromechanics, P.O. Box 3000, Espoo, FIN-02015.

the whole speed range. In practice, it has been seen that this performance objective is achieved, when the AMB open loop has a certain "shape". This means that the gain and phase margins are sufficient, the gain and phase crossover frequencies are suitable, the high frequency gain drops fast enough, the low frequency gain is high enough, etc. In SISO (single input single output) case these measures are readily seen from open loop frequency domain plots like Nyquist diagram, Bode diagram and Nichols chart. Also, these frequency response plots are useful in improving the design because the effect of controller modifications into the open loop frequency response is very straightforward. It is tempting to extend these methods to multivariable plants, because these methods have proven very useful, easy to use and intuitively clear in SISO case. In this paper, a new way of constructing a generalized Nyquist diagram is proposed and successfully used to design an AMB controller.

2 BEARING MAGNET ANALYSIS

In this Section, the behavior of the bearing magnets is analyzed. The analysis is concentrated on the parameters of the linearized bearing model. A minimum demand considering robustness is that the linearized system works well. The stability at large signal amplitudes is no less important and could be theoretically studied by simulations with a nonlinear model, and using describing function method. In the present paper, large signal amplitudes are consider only in the experimental testing.

In this paper, the finite element method is used to compute the linearized parameters (Antila et al. 1998a). Finite element method is reliable also with saturated magnetic circuit. In Figure 1, the bearing force is computed as a function of the control current for three different airgaps: 0.45 mm, 0.5 mm and 0.55 mm. These are considered as minimum, nominal and maximum airgap. The variations are due to the thermal enlargements and manufacturing tolerances. The small discrepancy between the measured and computed curves is due to material data.

The derivative of the bearing force with respect to control current is also shown in Figure 1. This is called current force coefficient. As seen, the current force coefficient depends considerably on the airgap and load. This is considered as the most important parameter variation in the AMB system. The nominal value is the mean of the maximum and minimum.

The negative stiffness coefficient has also quite high variations. From experience, it is known that under high load the rotor starts to oscillate at low frequency. This is due to the drop of the ratio between current force coefficient and negative stiffness coefficient. Thus, the nominal value for negative stiffness coefficient is chosen so that ratio between smallest current force coefficient (110 N/A) and nominal negative stiffness coefficient equals the correct ratio between these at the most loaded conditions. This leads to $k_P=1.3*10^6$ N/m.

The dynamic inductance L_{dyn} ($U=L_{dyn}*dI/dt$) decreases rapidly as the load increases. This is not so serious, because the fast current control loop effectively compensates the variations in the dynamic inductance. The uncertainty in the dynamic inductance can be described by small phase errors in the current force coefficient.

Large cross-connections between X-direction control current and Y-direction force, and vice versa, would obviously cause problems in the control. The authors have found out that the bearing pole configuration has a remarkable effect on this cross coupling and the NSNS-pole configuration is clearly better in this respect. In the NNSS-configuration, about 50 % cross-connection is present at the highly loaded condition. In the NSNS-configuration the cross-

connection is at worst about 15 %. A minor drawback with the NSNS-pole configuration are slightly higher friction losses, due to eddy currents. However, according to the measurements made by the authors, and others, this increase is small, only of the order of 10 %.

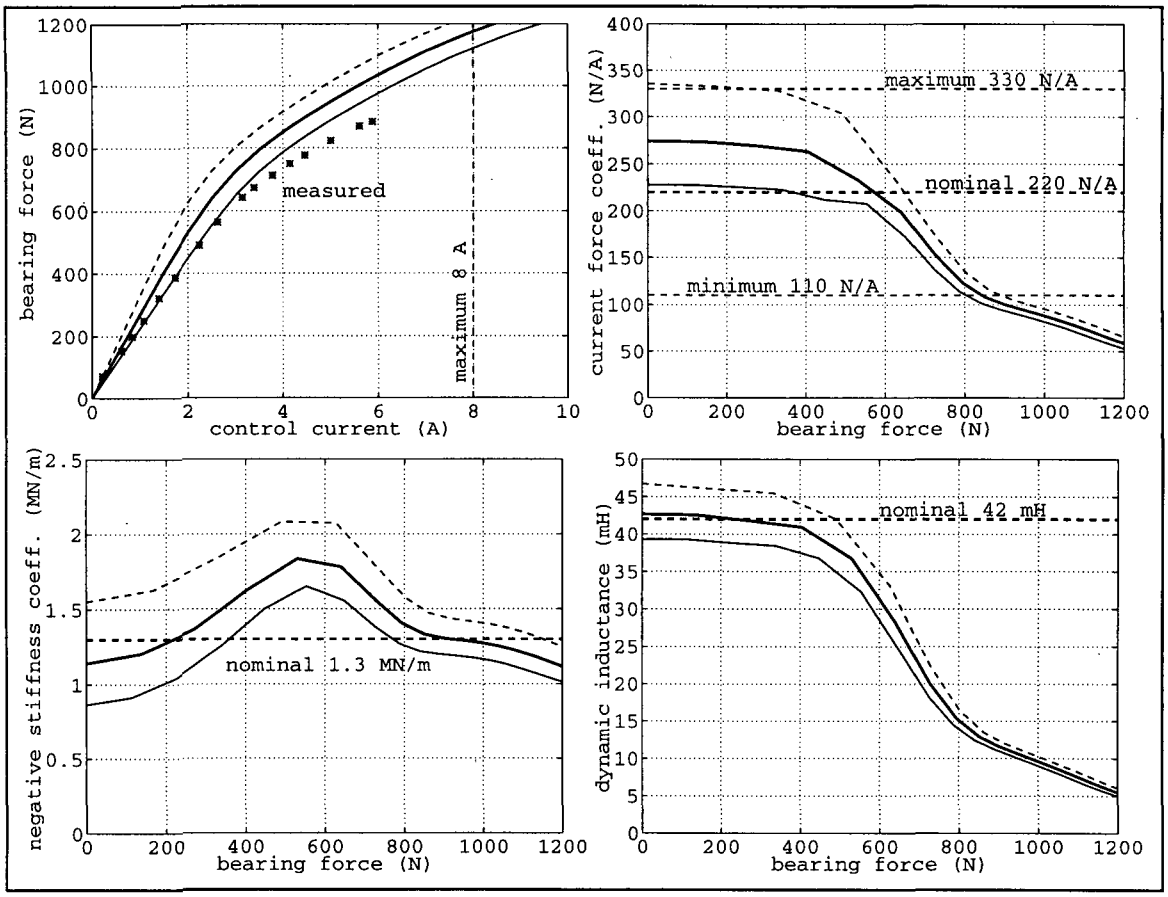

Figure 1. Current-force relationship and the linearized parameters with different airgaps and loads. Nominal airgap: bold line, small airgap: dotted line, large airgap: solid thin line.

3 THEORETICAL ROBUSTNESS ANALYSIS

The system layout for robustness analysis is shown in Figure 2.

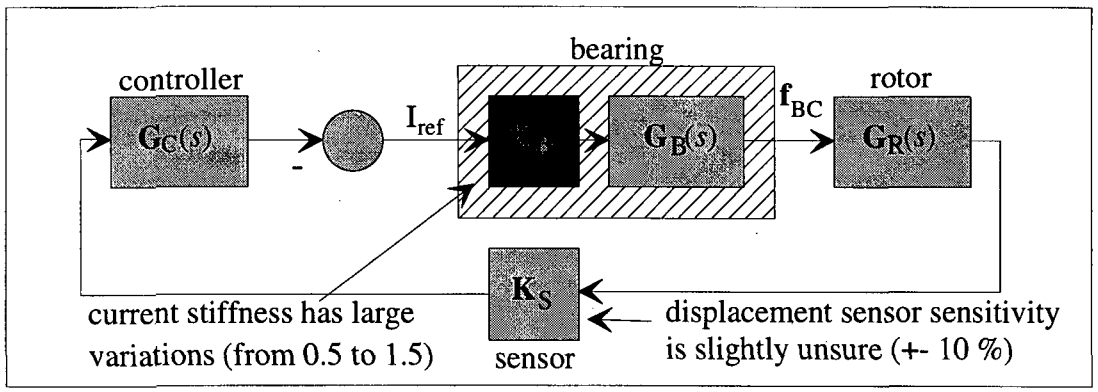

Figure 2. System layout for robustness analysis.

The displacement sensor is an inductive type sensor with excellent linearity and negligible cross-connections. The sensitivity is practically the same in one end X-and Y-directions, but may differ from its nominal value by 10 %, due to manufacturing process. So, $\mathbf{K}_S$ is a diagonal matrix, whose diagonal elements are real and in the range [0.9,1.1] and $k_{1,1}=k_{3,3}$ and $k_{2,2}=k_{4,4}$.

As seen in the last section, the bearing has a remarkable uncertainty, which can be described by an almost diagonal uncertain gain matrix $\mathbf{K}_B$. Based on the finite element analysis, the diagonal elements have absolute values in the range [0.5,1.5] and small phase. The eddy currents and hysteresis cause approximately 5° phase lag (Antila et al., 1998b) and the variations in the dynamic inductance may cause small phase lead or lag. Due to the magnetic cross-coupling, there are small nonzero elements in the locations (1,3), (3,1), (2,4) and (4,2).

METHODS FOR ROBUSTNESS ANALYSIS

For robustness analysis, the structured singular value (μ) is a powerful tool (originally introduced by Doyle 1982). Structured singular value is considered in many textbooks, see for example Maciejowski (1989), Skogestad and Postlethwaite (1996) and Zhou et al. (1997). By μ-analysis, very nonconservative statements can be made of the stability and performance robustness. In principle, there is no conservativeness, due to the definition of the μ and in practice the numerical upper bounds are close to the correct values. Today, reliable software exists for computing μ. The authors have used μ-analysis to check their designs and unquestionably it is a very useful and powerful tool. However, the authors have searched for a method, which would offer also some kind of quidance in the synthesis and intuitive feeling of when the design is good and still be nonconservative in the stability margin predictions.

As noted in the introduction, the open loop frequency response methods have proven very useful in SISO controller design. Also for multivariable case similar analysis and design methods have been developed. These "classical" frequency domain methods are collected in the book of Maciejowski (1989). Frequency domain stability analysis is based on the Generalized Nyquist criteria: Let the open loop transfer function matrix be $\mathbf{G}(s)$ (negative feedback convention). The closed system is stable if the characteristic loci of $\mathbf{G}(s)$ encircles -1 N_P times anticlockwise, as s encircles the right half plane. N_P is the number of right half plane poles of $\mathbf{G}$ and characteristic loci means a plot of the eigenvalues of $\mathbf{G}$ as a function of s.

The characteristic loci does not generally give any information of the robustness. It is difficult to predict how the characteristic loci will deformate when the parameters change. An obvious improvement is to compute at every frequency a template for every eigenvalue by changing the unsure parameters over their ranges. In practice, it may be difficult to compute these templates, especially, as the borders of the templates are not in general achieved at bounding parameter values. If the system is diagonally dominant, a generalized Nyquist-diagram with Gerschgorin bands may be useful. There is also a method for finding a diagonal scaling matrix that gives optimally thin Gerschgorin bands (Mees 1981). Postlethwaite et al. (1981) proposed principal phases to be used with principal gains to draw "principal regions" into the Nyquist-diagram. Then, certain robustness statements can be made.

The authors have tested all the previous methods in the case of AMB. Sometimes the methods are useful, but often the predictions will be too conservative. For example, some AMB systems have very small offdiagonal elements. In such case, the Nyquist-plot with Gershgorin bands is useful, giving highly nöncorservative results. Generally, the nondiagonal elements are not small and they can not be made small by diagonal scaling. It seems to be that

in a well designed AMB system the open loop is not necessarily diagonal near the cross-over frequencies, but it is near normal (matrix **A** is called normal if $\mathbf{A}^H\mathbf{A}=\mathbf{A}\mathbf{A}^H$). Even though the normality is considered as a nice property of a control loop (Maciejowski 1989), it is not so obvious what is the actual benefit in the case of AMB. Actually, this conclusion can be made just after quite tedious analysis. Only the main ideas are explained in the following.

For normal matrix the largest and smallest singular values are the largest and smallest absolute values of its eigenvalues and with skew matrix they are bigger and smaller, respectively. In a multivariable plant, the closed loop eigenvalues are not a good measure of performance, but the singular values are. By some analysis, it can be found out that near the gain and phase cross-over frequencies, the largest singular values of the sensitivity function and the complementary sensitivity functions at the plant input and output are good measures of performance. None of these should not become too high. As the closed loop frequency response functions are normal if and only if the open loop is normal, the largest singular values are easiest to keep small when the open loop is normal. Because the open loop eigenvalues suffer from the same phase-gain relationships as the gain and phase of a scalar plant, it will be difficult to compensate the lost performance by shaping the characteristic loci. Further, normal open is optimal considering robustness against certain type of perturbations.

NEW GENERALIZED NYQUIST DIAGRAM

Let **K** be the unsure, almost diagonal gain matrix and $\mathbf{L}_0$ the nominal open loop frequency response matrix (negative feedback convention). The open loop frequency response matrix is then $\mathbf{K}\mathbf{L}_0$ and the eigenvalues of the open loop are obtained from the eigenvalue problem

$$\mathbf{K}\mathbf{L}_0\mathbf{v}_n = \lambda_n\mathbf{v}_n\,, \tag{1}$$

where λ_n is an eigenvalue and $\mathbf{v}_n$ is the corresponding eigenvector. Equation 1 is now multiplied from left by $\mathbf{K}^{-1}$ and $\mathbf{v}_n^H$ and divided by $\mathbf{v}_n^H\mathbf{K}^{-1}\mathbf{v}_n$. This leads to

$$\lambda_n = \frac{\mathbf{v}_n^H\mathbf{v}_n}{\mathbf{v}_n^H\mathbf{K}^{-1}\mathbf{v}_n}\frac{\mathbf{v}_n^H\mathbf{L}_0\mathbf{v}_n}{\mathbf{v}_n^H\mathbf{v}_n}\,, \tag{2}$$

where $\mathbf{v}_n^H\mathbf{L}_0\mathbf{v}_n / \mathbf{v}_n^H\mathbf{v}_n$ is called Rayleigh fraction in the literature. The idea is to use Equation 2 to estimate, where the open loop eigenvalues travel when the matrix **K** varies. The problem is that we do not know how the eigenvectors behave when **K** changes. Because of that the vector $\mathbf{v}_n$ is allowed to be any vector **x**, not necessarily an eigenvector. Then we can say that

$$\begin{aligned}
&\lambda_n \in \left\{ab,\ a\in\varphi(\mathbf{L}_0),\ b\in\phi\left(\mathbf{K}^{-1}\right)\right\},\ \varphi(\mathbf{L}_0)=\left\{\frac{\mathbf{x}^H\mathbf{L}_0\mathbf{x}}{\mathbf{x}^H\mathbf{x}},\ \mathbf{x}\in\mathbf{C}^{N\times 1}\ \mathbf{x}\neq\mathbf{0}\right\},\\
&\phi(\mathbf{K})=\left\{\frac{\mathbf{x}^H\mathbf{x}}{\mathbf{x}^H\mathbf{K}^{-1}\mathbf{x}},\ \mathbf{x}\in\mathbf{C}^{N\times 1}\ \mathbf{x}\neq\mathbf{0},\mathbf{K}\in\{\text{"allowed variations"}\}\right\},
\end{aligned} \tag{3}$$

where $\varphi(\mathbf{L}_0)$ is called the eigenvalue region of $\mathbf{L}_0$ and $\phi(\mathbf{K})$ is called the gain set of **K**.

It is relatively easy to prove that $\varphi(\mathbf{A})$ is a convex set in the complex plane. This convexity property is useful in computing the region numerically. Tangent lines are computed in a number of directions α (see Figure 3). To obtain the upper and lower tangent lines, compute a hermitic matrix $\mathbf{P} = \left(e^{-i\alpha}\mathbf{L}_0 + e^{i\alpha}\mathbf{L}_0^{\mathrm{H}}\right)/2$. Then a and b (see Figure 3) are the most negative and positive eigenvalues of $\mathbf{P}$, respectively. To get an accurate approximation, about 20 angles between -90° .. 90° is enough. From these tangent lines, the approximation of the region can be constructed. A remarkable property of the eigenvalue region is that if matrix $\mathbf{A}$ is normal then the region $\varphi(\mathbf{A})$ is bounded by line segments connecting the outmost eigenvalues of $\mathbf{A}$. This is illustrated in Figure 3. The plot of these eigenvalue regions $\varphi(\mathbf{L}_0)$ at a sufficient number of frequency points is the generalized Nyquist-diagram proposed in this paper.

Let us next analyze, how does the gain set $\phi(\mathbf{K})$ look like. If the matrix $\mathbf{K}$ is diagonal, with real diagonal elements limited in the interval [c,d], then $\phi(\mathbf{K})$=[c,d]. In the case of AMB, the postulated variation range is between 0.5 and 1.5. If $\mathbf{K}$ is diagonal, but its elements have small phase errors, then the maximum phase of the elements of $\phi(\mathbf{K})$ equals the maximum phase of the diagonal elements. Let $\mathbf{K}$ be a real 2×2 matrix, with positive diagonal elements and small offdiagonal elements. If the absolute value of the larger offdiagonal element is smaller than k*smaller of the diagonal elements then the maximum absolute value of the phase of the members of $\phi(\mathbf{K})$ is argtan(k). Thus, 15 % cross-connection means at maximum 8.5° phase. A physical explanation for this phase angle is that the cross-connections modify the spatial phase of a rotating force vector. Note that $\mathbf{K}_\mathrm{B}$ consists of two 2×2 blocks, so the previous reasoning holds for $\mathbf{K}_\mathrm{B}$. The gain set $\phi(\mathbf{K}_\mathrm{B})$ is sketched in Figure 3.

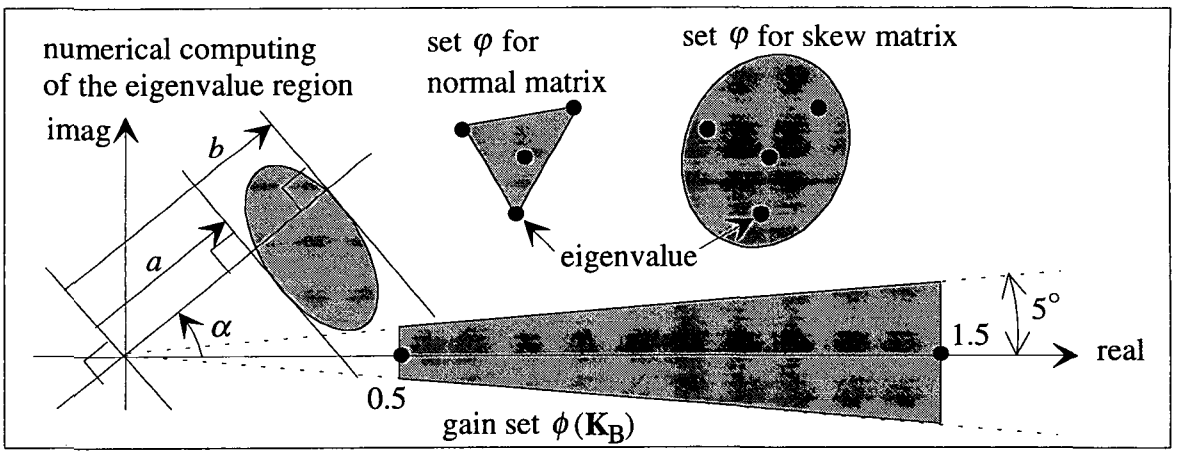

Figure 3. Numerical computing of the eigenvalue region φ and a example region for normal and skew matrix. In the real axis the gain set $\phi(\mathbf{K}_\mathrm{B})$ is shown.

As the matrix $\mathbf{L}_0$ is not necessarily normal, a question arises, whether it is possible to find a similarity transformation $\mathbf{D}$ that would make it more normal. It is easy to see that $\rho[\mathbf{K}\mathbf{L}_0] = \rho\left[\left(\mathbf{D}\mathbf{K}\mathbf{D}^{-1}\right)\left(\mathbf{D}\mathbf{L}_0\mathbf{D}^{-1}\right)\right]$ where $\rho[\mathbf{A}]$ means the set of the eigenvalues of $\mathbf{A}$. Let us introduce a "structured" eigenvalue region as follows

$$\varphi_S(\mathbf{L}_0)=\left\{\cap\left\{\frac{\mathbf{x}^H\mathbf{D}\mathbf{L}_0\mathbf{D}^{-1}\mathbf{x}}{\mathbf{x}^H\mathbf{x}},\ \mathbf{x}\in\mathbf{C}^{N\times 1}\ \mathbf{x}\neq\mathbf{0}\right\},\mathbf{D}\in\text{"allowed scalings"}\right\},\tag{4}$$

where "allowed scalings" is a set of invertible matrices, which commutes with all allowed **K**:s, i.e. **KD=DK**, or $\mathbf{K}=\mathbf{DKD}^{-1}$. The eigenvalue region can be replaced by this structured eigenvalue region, if the conservativeness should be minimized.

The computing of this structured eigenvalue region is more tedious than the original version and in the case of many free parameters in **D** it is quite difficult (it comes very close to μ-computing). However, in the present case we demand that $d_{1,1}=d_{3,3}$ and $d_{2,2}=d_{4,4}$, because $\mathbf{K}_B$ has small off-diagonal elements. Further, we can set $d_{1,1}=d_{3,3}=1$, because multiplying the matrix **D** by a constant does not change matrix $\mathbf{DXD}^{-1}$. So, we have only one free parameter $d=d_{2,2}=d_{4,4}$, which can be further restricted to be real positive number.

The small uncertainty in the sensor sensitivity is taken into consideration by computing the union of the eigenvalue regions $\varphi(\mathbf{G}_C\mathbf{K}_S\mathbf{G}_R\mathbf{G}_B)$ when $\mathbf{K}_S$ achieves all allowed variations. As this union is no more convex, it is approximated by the smallest convex region containing it. This is not so tedious, because the sensor sensitivity can be parametrized by two real parameters and the Rayleigh fraction building the eigenvalue region is then a linear combination of these parameters. So, it suffices to compute the smallest convex region that contains the four regions achieved with the four bounding parameter combinations.

4 ANALYZING THE TEST MACHINE

The proposed generalized Nyquist diagram was used to analyze the test machine. In the computations, a ± 10 % variation was assumed for the displacement sensor sensitivity. In Figure 4, the Nyquist diagrams for zero and maximum speeds are shown. Only the positive frequencies are drawn, because the diagram is symmetric relative to real axis. The circle in Figure 4 is centered in −1 and its radius is 0.5. It is a kind of a performance circle. To achieve good performance, the regions should not penetrate inside the circle too much. From Figure 4 the designer sees that the control system is tolerable, but not the best possible. At frequencies near the bending mode the structured version is used to decrease the conservativeness.

At zero speed, the system tolerates 50 % decrease in the current stiffness. The test machine has the current stiffness very near the nominal value as can be seen in Figure 1. The drop in the current stiffness was simulated by dropping the controller gain at the controller output. In practice, the system tolerated exactly 50 % drop. However, the machine could be run over the rigid body resonances, just after the gain was more than 70 % of the nominal. At lower values the vibrations caused by electric motor became too high at low speed. This can be predicted from Figure 4. If the Nyquist-curve is scaled by 0.7, it will go clearly inside the performance circle. So, the static gain of the control loop should be increased about 50 %.

Then we tested the increase in the gain. The Nyquist-curve predicts that the system tolerates slightly more 100 % increase. In practice, we could increase the gain by 120 %. However, with more than 100 % increase the rotor started violently oscillating when hammered. So, the system was no more stable in large signal amplitudes. This effect is due to power amplifier saturation and is studied in detail by Satoh et. al (1990). With more than 80 % increase, amplifier saturation occurred when the machine was driven over rigid body resonance speeds.

Again, this can be predicted from the Nyquist-diagram. If the curve is scaled by 1.8, it will penetrate clearly inside the performance circle.

So, we should increase the controller gain at low frequencies and slightly decrease the gain at the phase cross-over frequency. The Nyquist-diagram reveals that this is difficult to achieve with the present controller structure, because the eigenvalue regions are oblong and pointing to origin. To get the closest point far enough from the origin at low frequencies, the furthest point goes very far. To improve the design, we should separate the controller into translatory and rotary mode controllers. Then we would have direct access to both eigenvalues.

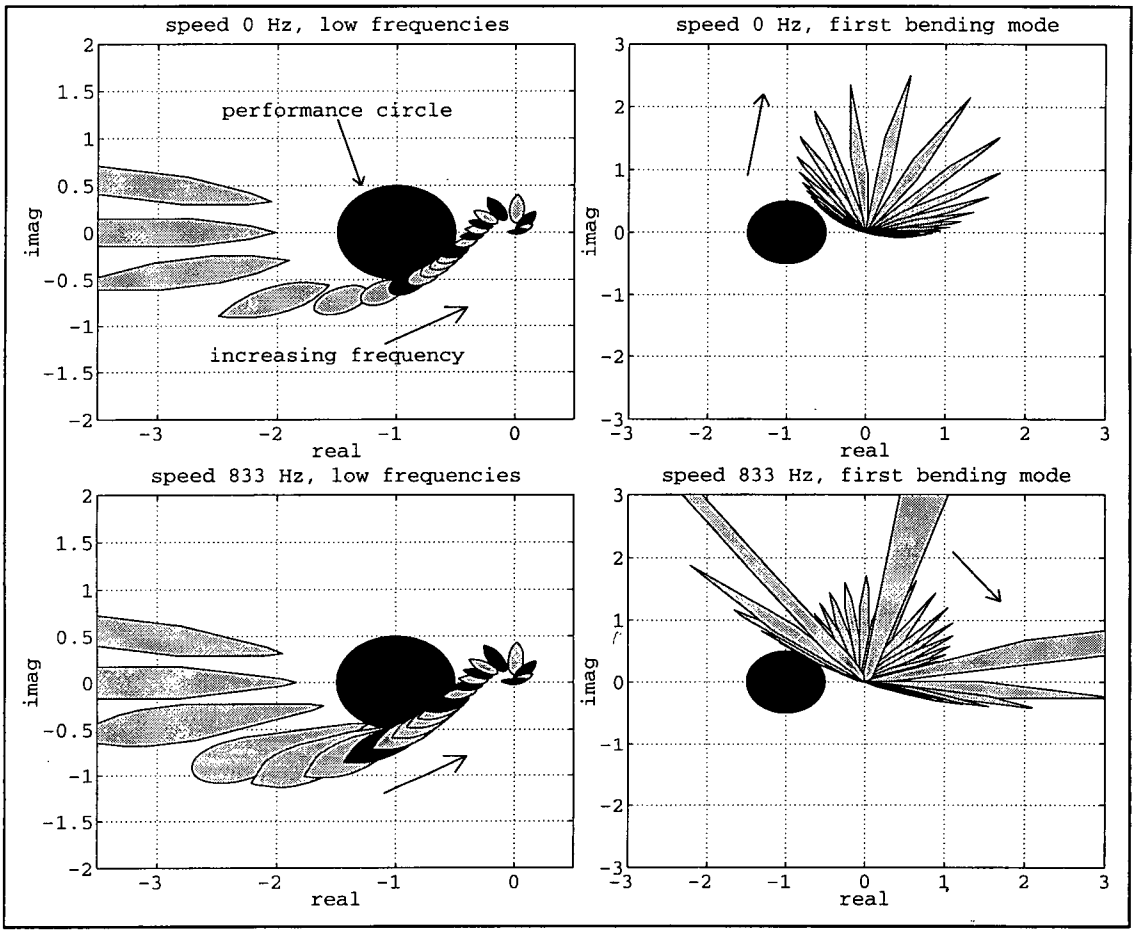

Figure 4. Generalized Nyquist diagram for the test machine. At the left, the diagram is drawn for low frequencies: 5, 10, 20, 40, 60, 80, 100, 120, 140, 160, 180, 200, 250, 300, ... 800 Hz. The exact hundreds are filled with black. In the right hand side plots, the frequency range was from 800 Hz to 1100 Hz with 1 Hz step.

The first bending mode is stable at zero speed and both the forward and backward modes are stable at maximum speed. The size of the curves near the bending mode depends on the modal damping, which was assumed 0.003. However, the system remains stable even if the damping is smaller. However, a 30° phase lead at the bending eigenfrequency could destabilize the bending mode. This phase lead could be due to decrease in the dynamic inductance at high loads. So, the controller phase should be dropped slightly lower at the bending mode eigenfrequency. With the present controller structure it may be difficult to achieve. To adjust the phase more effectively, we should introduce a complex pole zero pair into the controller.

5 CONCLUSIONS

When designing AMB system for series production, a special attention has to be put on the robustness. The designer has to find out how the process dynamics may be changing due to operational conditions and manufacturing tolerances. It was found that the most remarkable uncertainty is the current force coefficient. The uncertainty can be described by an almost diagonal and real gain matrix. For theoretical analysis, a special generalized Nyquist-diagram was proposed. This diagram is a nice generalization of the SISO-Nyquist-diagram. It gives highly nonconservative robustness estimates in the case of AMB and serves as a synthesis tool. The theoretical analysis based on a linearized model is a kind of minimum demand. In experimental testing these stability limits should be checked also with high signal amplitudes.

REFERENCES

Antila M., Lantto E., Saari J., Esa H., Lindgren O., Säily K. 1996. "Design of Water Treatment Compressors Equipped with Active Magnetic Bearings". Fifth International Symposium on Magnetic Bearings. Kanazawa, Japan, pp. 389-394.

Antila, M. Lantto E. Arkkio A. 1998a. "Determination of Forces and Linearized Parameters of Radial Active Magnetic Bearings by Finite Element Technique". Accepted on IEEE *Transactions on Magnetics* 1998.

Antila M., Lantto E., Tommila V. 1998b. "Determination of Eddy Current Effects on Radial Active Magnetic Bearings Based on a Reluctance Network and 1D Eddy current Model". Proceedings of the 6th ISMB, Boston, USA.

Doyle J.C. 1982. "Analysis of feedback systems with structured uncertainties". *IEE proceedings*, Part D, 129(6), pp. 242-250.

Fittro R. L., Knospe C.R., Stephens L.S. 1996. "Experimental Results of μ-Synthesis Applied to Point Compliance Minimization". Fifth International Symposium on Magnetic Bearings. Kanazawa, Japan, pp. 203-208.

Lantto E. 1997. "Finite Element Model for Elastic Rotating Shaft". *Acta Polytechnica Scandinavica*. Electrical Engineering Series No. 88. 73 p.

Maciejowski, J.M. 1989. "Multivariable Feedback Design". Addison-Wesley. 424 p.

Mees A.I. 1981. "Achieving Diagonal Dominance". *System and Control Letters*, 1, 155-158.

Postlethwaite I., Edmunds J. M., McFarlane A. 1981. "Principal Gains and Principal Phases in the Analysis of Linear Multivariable Feedback Systems". *IEEE Transactions on Automatic Control*, 26, No.1, pp. 32-46.

Satoh I., Murakami C., Nakajima A., Kanemitsu Y. 1990. "A Self-Exited Vibration of Magnetic Bearing System with Flexible Structure". 2nd International Symposium on Magnetic Bearings, Tokyo, Japan, pp. 329-335.

Skogestad S., Postlethwaite I. 1996. "Multivariable Feedback Control". John Wiley & Sons Ltd., England. 559 p.

Zhou K., Doyle J.C., Glover K. 1997. "Robust and Optimal Control". Prentice-Hall Inc. 596 p.

APPENDIX: PARAMETERS OF THE TEST MACHINE

The test machine is a 100 kW 50000 1/min. air compressor prototype for waste water treatment. The rotor mass is 40 kg and motor diameter 115 mm. The radial magnetic bearings are conventional 8-pole bearings. Stator packet length is 50 mm, outer diameter 180 mm and slot diameter 150 mm. Rotor diameter is 74 mm, shaft diameter 53 mm and nominal airgap 0.5 mm. Number of turns is 100 per pole and pole configuration is NSNSNSNS. Bias current is 2 A, amplifier maximum current 10 A and amplifier voltage 150 V. Static load capacity is 850 N in weakest direction, the nominal current force coefficient is k_C=220 N/A, the nominal negative stiffness coefficient is k_P=1.3*10^6 N/m and the nominal dynamic inductance is L_{dyn}=42 mH. The bearing model is

$$\mathbf{f}_{BC}(s) = \mathbf{G}_B(s)\mathbf{I}_{ref}(s),\ \mathbf{G}_B(s) = \mathrm{diag}\{G_{B1}, G_{B1}, G_{B1}, G_{B1}\},\ G_{B1}(s) = \frac{k_C k_I}{L_{dyn}s + k_I}, \quad \text{(A1)}$$

where k_I is the current feedback coefficient =75 V/A, $\mathbf{I}_{ref}$ is the reference control current and $\mathbf{f}_{BC}$ is the controlled bearing force. The rotordynamic model is

$$\mathbf{p}_S(s) = \mathbf{G}_R(s)\mathbf{f}_{BC}(s)$$

$$\mathbf{G}_R(s) = \begin{bmatrix} \mathbf{C}_S & \mathbf{0} \\ \mathbf{0} & \mathbf{C}_S \end{bmatrix} \begin{bmatrix} \mathbf{M}s^2 + \mathbf{D}s + \mathbf{K} - \mathbf{B}_b k_P \mathbf{B}_b^T & \Omega\mathbf{G}s + \Omega\mathbf{D} \\ -\Omega\mathbf{G}s - \Omega\mathbf{D} & \mathbf{M}s^2 + \mathbf{D}s + \mathbf{K} - \mathbf{B}_b k_P \mathbf{B}_b^T \end{bmatrix}^{-1} \begin{bmatrix} \mathbf{B}_b & \mathbf{0} \\ \mathbf{0} & \mathbf{B}_b \end{bmatrix} \quad \text{(A2)}$$

where $\mathbf{p}_S$ is the position measurement vector. The rotordynamic matrices are

$$\mathbf{M} = \mathrm{diag}\{40.7, 1.22, 0.99\},\ \mathbf{K} = \mathrm{diag}\{0, 0, 37.5*10^6\},\ \mathbf{D} = \mathrm{diag}\{0, 0, 35\},$$

$$\mathbf{G} = \begin{bmatrix} 0 & 0 & 0 \\ 0 & 55 & 0.86 \\ 0 & 0.86 & 145 \end{bmatrix} *10^{-3},\ \mathbf{B}_b = \begin{bmatrix} 1 & 1 \\ 0.26 & -0.27 \\ 0.084 & 0.17 \end{bmatrix},\ \mathbf{C}_S = \begin{bmatrix} 1 & 0.30 & 0.25 \\ 1 & -0.31 & 0.27 \end{bmatrix}. \quad \text{(A3)}$$

For details of the rotordynamic model, see Lantto (1997). The position controller is

$$\mathbf{I}_{ref}(s) = \mathbf{G}_C(s)\mathbf{p}_S(s),\ \mathbf{G}_C(s) = \begin{bmatrix} \mathbf{G}_{C1}(s) & \mathbf{0} \\ \mathbf{0} & \mathbf{G}_{C1}(s) \end{bmatrix},\ \mathbf{G}_{C1}(s) = \begin{bmatrix} 1 & 0.36 \\ 0.36 & 1 \end{bmatrix} \begin{bmatrix} G_{C2}(s) & 0 \\ 0 & G_{C2}(s) \end{bmatrix},$$

$$G_{C2}(s) = \left[18300\left(1 + \frac{1}{0.15s}\right) + \frac{40s}{0.0002s + 1}\right]\left[\frac{3500^2}{s^2 + 1050s + 3500^2}\right]. \quad \text{(A4)}$$